

Hybrid materials based on Fe₂O₃/metal-oxide reinforced polyaniline: Synthesis, characterization and their electrochemical properties

Fatima Zohra Zeggai, Ilyes Otmane, Hafida Zerigui, Redouane Chebout and Khaldoun Bachari

Abstract– Polyaniline (PANI)-Fe₂O₃/CuO and PANI -Fe₂O₃/ZnO hybrid materials were developed and prepared by in situ polymerization at 0°C using ammonium persulfate as oxidant. The resulting products are investigated for their structural properties by X-ray diffraction (XRD), Fourier transform infrared (FTIR), and scanning electron microscopy (SEM), and the results confirm the formation of the hybrid architecture. In addition, the electrochemical properties of the hybrid products are investigated by cyclic voltammetry (CV) and optical properties were determined using UV-Vis Diffuse Reflectance Spectrophotometer (UV-Vis DRS). Compared to PANI/ZnO or CuO, Fe₂O₃/CuO or ZnO exhibit significantly improved properties. Based on the obtained results, the products thus open the way for a variety of electrical and sensors applications.

Keywords– Polyaniline, metal oxide, in-situ polymerization, hybrid material, electrochemical properties.

NOMENCLATURE

PANI	Polyaniline.
APS	Ammonium persulfate.
XRD	X-ray diffraction.
FTIR	Fourier transform infrared.
SEM	Scanning electron microscopy.
UV-vis	Ultraviolet-visible spectroscopy
CV	Cyclic Voltammetry.
ECPs	Electronically conducting polymers
CuO	Copper oxide
ZnO	Zinc oxide
JCPDS	Joint Committee of Powder Diffractions Standards

I. INTRODUCTION

Electronically conducting polymers (ECPs) continue to be of great interest and importance as components for promising applications in energy storage, electrocatalysis, organic electrochemistry, bioelectrochemistry, photoelectrochemistry, electroanalysis, sensors, microsystems engineering, electronic devices, microwave shielding and corrosion protection, etc. Polymeric materials and their composites are capable of changing their structure and properties during reaction with

Manuscript received February 8, 2023; revised April 9, 2023.

F.Z. Zeggai, R. Chebout and K. Bachari are with the materials chemistry division, Scientific and Technical Research Center in physico-chemical analyses CRAPC, Bou-ismail Tipaza, ALGERIA (e-mail: zeggai.fatimazohra@crapc.dz, rchebout@crapc.dz, khaldoun.bachari@crapc.dz).

I.Otmane is with the Research laboratory on physico-chemistry of surfaces and interfaces (LRPCSI), University of August 20, 1955-Skikda, ALGERIA and the polymer chemistry laboratory (LCP), University of Ahmed Ben-Bella Oran1, ALGERIA (e-mail: i.otmane@univ-skikda.dz).

H. Zerigui is with the polymer chemistry laboratory (LCP), University of Ahmed Ben-Bella Oran1, ALGERIA, (e-mail: dida-hafida@hotmail.com).

the environment. Among conducting polymers, polyaniline (PANI) exhibits excellent electrical conductivities and thermal stability [1-2]. It has promising applications in various technological fields such as energy storage [3], electronic and optical devices [4], sensors [5-6], corrosion protection [7] and many more [8-9].

Several studies have been conducted on conductive polymers hybridized with metal oxides to produce functional nanomaterials with excellent properties not only for their intriguing structural characterization but also for their potential functional applications in advanced technologies, such as adsorption, separation, gas storage, antistatic coatings, electrochemical displays, sensors, catalysis, redox capacitors, electromagnetic shielding, etc. Understanding the interactions between the polymer matrix and the metallic filler is essential for the technological implementation of synthesis and engineering of hybrid structures with different dimensions, collective properties at the micro/nanoscale, and predictable physical and mechanical responses to the polymer-metal filler interface. The concept of hybridizing the properties of nanocomposites to form an extraordinary nanomaterial (with the advantages that are not just the sum of the individual contributions) is a famous, renowned technology. Current studies mostly focus on binary metal oxides because they have complementary properties, such as TiO₂, Fe₂O₃, ZnO, ZrO₂, V₂O₅, NiO and Al₃O₄ have been widely studied as nanomaterials for semiconductors [10-14]

The aim of this work was to prepare various hybrid materials PANI /CuO, PANI /ZnO, PANI-Fe₂O₃/CuO, PANI -Fe₂O₃/ZnO by in situ polymerization method using ammonium persulfate as oxidant and to investigate the effects of metal oxides on the surface morphology and properties of PANI. It is also important to find an optimal value for the addition of metal oxide to obtain a perfect hybrid nanomaterial. The organic-inorganic materials were confirmed by various analyses such as: XRD, FT-IR, SEM and UV-vis. The electrochemical behaviour was investigated by cyclic voltammetry. Moreover, the results could be promising for the fabrication of new functional materials, such as organic devices based on metal oxide integrating conducting polymers.

Digital Object Identifier (DOI): 10.53907/enpesj.v3i1.181

II. METHODOLOGY

II.1. Apparatus

Fourier Transform Infrared (FT-IR) spectroscopy spectra were recorded using Alpha Bruker. The scanning was performed between 4000 and 400 cm⁻¹ for 32 times with a resolution of 4 cm⁻¹. All spectra were baseline-corrected with Opus software.

The X-ray diffraction (XRD) patterns were recorded on a Bruker D8 Advance diffractometer DAVINCI model, operating in Bragg–Brentano geometry, with anode using Cu K α as radiation source ($\lambda = 1.5418 \text{ \AA}$).

The ultraviolet–visible diffuse reflectance spectra measurements were recorded using a SPECORD 210 PLUS - 223F1138 UV-Vis spectrophotometer.

Electrochemical properties were carried out using a conventional cell of three electrodes. The counter and reference electrodes were a platinum foil and a hydrogen reversible electrode (RHE), respectively. The entire electrochemical test was carried using the Dimethyl Sulfoxide (DMSO), 50 μL of this solution were cast over graphite carbon electrodes and the solvent evaporated to create polymeric films. The electrolyte used was tetrabutylammonium hexafluorophosphate (TBAPF₆) and all experiments were carried out at 50 mV/s.

Scanning Electron Microscopy (SEM) analysis of nanocomposites powder was performed on a Quanta FEG 250 instrument (FEI, Hillsboro). A tiny amount of material should be collected with a spoon and allowed to fall on a carbon or aluminium holder. Excess particles should then be sprayed away, and the sample should then be coated for imaging.

II.2. Materials

The Aniline monomer employed for the polymerization reaction, ammonium persulfate (APS), copper oxide (CuO, black powder, purity 99%), zinc oxide (ZnO, white powder, purity 99%) were obtained from the company Sigma Aldrich. Di-iron trioxide (Fe₂O₃, reddish powder, purity 95-98%) was purchased from Biochem-Chemopharma. Sulfuric acid was purchased from Merck. All solutions were prepared with distilled water.

II.3. Preparation of the PANI/CuO, PANI/ZnO, PANI-Fe₂O₃/CuO, PANI -Fe₂O₃/ZnO hybrid nanocomposites

Polyaniline/(CuO or ZnO) samples were prepared by in situ oxidative polymerization. In a typical experimental procedure, the polymerization reaction was carried out at 0°C. The amount of CuO or ZnO (1%, 3%, and 5% of the molar weight of the aniline monomer) was added to the aniline monomer (0.022 M) in a 100-ml flask, followed by an oxidizing solution of ammonium persulfate (0.022M) with drop wise aqueous solution of H₂SO₄ (1 M), and the mixture was stirred for 24 hours. PANI-Fe₂O₃/CuO, PANI -Fe₂O₃/ZnO hybrid samples were prepared in the same manner as the previous samples, with Fe₂O₃ (0.5 g) added to all of them.

III. RESULTS AND DISCUSSION

III.1. Vibrational characterization by FT-IR spectroscopy

The representative FT-IR spectra of all samples were given in Figs.1, 2, and 3. The polymerization reaction of aniline is

initiated by an external oxidizing agent (APS) and combined with metal oxide such as CuO or ZnO as Fe₂O₃.

Evidence for the polymerization of aniline is provided by FT-IR spectroscopy. For comparison, a bulk polyaniline was first synthesized by the same method used for composites (in-situ). 0.2 ml (220 mmol) of aniline was added to 0.49 g (220 mmol) of ammonium persulfate in 100 ml of distilled water, then 5 ml of 1M H₂SO₄ was added dropwise to the previous solution. The mixture was stirred at 0°C for 24 hours and finally filtered, washed with distilled water and dried at room temperature. The FT-IR spectrum of polyaniline in Fig.3 exhibits the characteristic peaks found at 3491-3426, 2361, 1544, 1440, and 1284 cm⁻¹ are assigned to N-H stretching, C=N stretching, the ring mode of quinoid structures, the benzoid structure, and C-N stretching of secondary aromatic amine respectively [15-17].

The FT-IR spectra of Pani/CuO and Pani/ZnO at (3, 5, and 7%) are shown in Figs.1 and 2. The FT-IR spectra of the samples show the characteristic vibrations of polyaniline, which agree well with those of chemically synthesized polyaniline. The observed main peaks in the range 411-876 cm⁻¹ characterize the Zn-O-Zn and Zn-O stretching [18]. Samaele et al [19] and Prasad et al [20] reported similar FT-IR spectra of zinc oxide nanoparticles in their studies. For CuO nanoparticles, the absorption bands in the low frequency region of spectra located in the range 553-794 cm⁻¹ confirm the successful deposition of copper oxide [21]. In addition, one other characteristic peak of CuONPs was observed at 1551 cm⁻¹ shows the Cu–O symmetrical stretching.

Figs.1 and 2 shows the FT-IR spectra of the ternary hybrid materials PANI-Fe₂O₃/CuO, PANI-Fe₂O₃/ZnO. The peak of 1518 cm⁻¹ and 1639 cm⁻¹ represent C-C stretching between quinone ring (Q) and benzene ring (N) on PANI, respectively. The absorption band at 1215 cm⁻¹ is C-N stretching of benzene ring, while the peak at 1088 cm⁻¹ is attributed to C-H bending vibration [22]. However, in the PANI-Fe₂O₃/CuO these peaks are small and intense, perhaps due to the effect of Fe₂O₃ on the samples. The presence of copper and zinc oxides was confirmed by their characteristic peak. Two very intense absorption peaks at 517 cm⁻¹ and 434 cm⁻¹ can be distinguished, corresponding to Fe-O bonds in iron oxide. This might be attributed to the strong mutual interactions of hydrogen bonding between the Fe–O of Fe₂O₃ and N-H group of PANI [23].

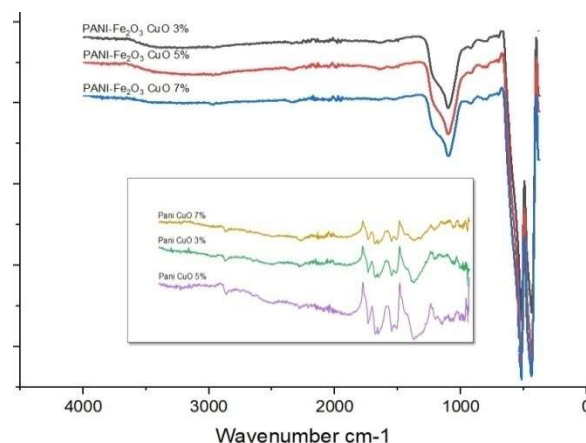


Fig. 1: FT-IR spectra of the Pani-CuO (3%,5%,7%), and hybrid nanocomposites Pani-Fe₂O₃/CuO (3%,5%,7%).

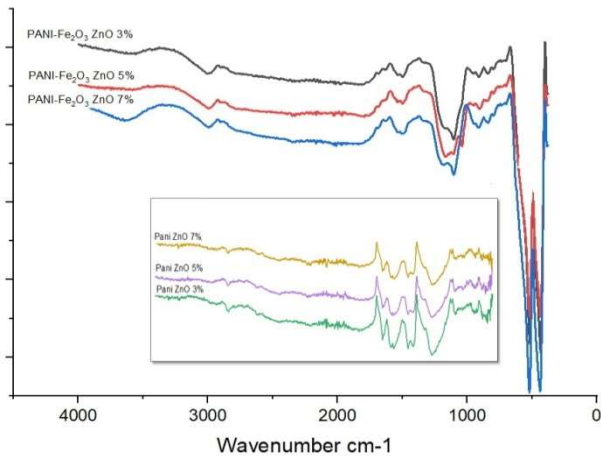


Fig. 2: FT-IR spectra of the Pani- ZnO (3%,5%,7%), and hybrid nanocomposites Pani-Fe₂O₃/ZnO (3%,5%,7%).

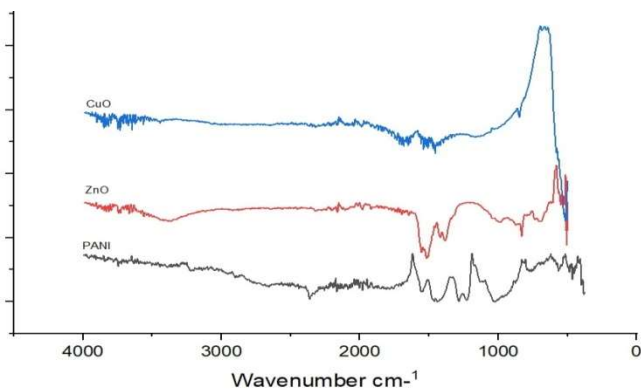


Fig. 3: FT-IR spectra of copper oxide, zinc oxide and Polyaniline.

III.2. XRD spectroscopy

The XRD patterns of ZnO, CuO, and Fe₂O₃ nanoparticle, pure PANI and PANI/CuO, PANI/ZnO, PANI-Fe₂O₃/CuO, PANI-Fe₂O₃/ZnO nanocomposites with the different loading amount of ZnO and CuO (3, 5, and 7%) were shown in Figs.4, 5, and 6.

The bulk PANI XRD diagram is shown in Fig.4. The PANI peak diffracted at an angle of $2\theta = 20.43^\circ$ and $2\theta = 25.27^\circ$ with a d-spacing of 4.35 Å and 3.52 Å, respectively, corresponding to the (200) and (101) planes. The figure shows the low crystallinity of polyaniline due to the repetition of benzenoid and quinoid rings in its chains [24].

The analysis of XRD pattern of ZnO shows the characteristics peaks at $2\theta = 31.84^\circ, 34.52^\circ, 36.38^\circ, 47.64^\circ, 56.70^\circ, 63.06^\circ, 68.10^\circ,$ and 69.18° corresponding to crystal planes (100) (002) (101) (102) (110) (103) (112) and (201), respectively, were associated with the hexagonal crystal structure of ZnO. All diffraction peaks are in agreement with those of the wurtzite hexagon structure of ZnO prepared [25]. The values given for ZnO are related to JCPDS #36-1451. It also confirms that the nanoparticle produced was free of impurities because it does not contain characteristic peaks other than those of zinc oxide [26].

The characteristics peaks of CuO comes at $2\theta = 32.49^\circ, 35.56^\circ, 38.68^\circ, 46.23^\circ,$ and 48.76° correspond to crystal planes (110), (-111), (200), (-112), and (-202), respectively. The intensities and positions of the observed diffraction peaks agree well with those published in JCPDS #41-0254. This result suggests that we have a single phase of CuO with a monoclinic structure, which is consistent with the literature [27]. The profiles of the main diffraction peaks reflect the high degree of crystallinity of the synthesized CuO particles. No

other phases such as Cu₂O and Cu(OH)₂ were observed, which means that the prepared powder is CuO with very high purity.

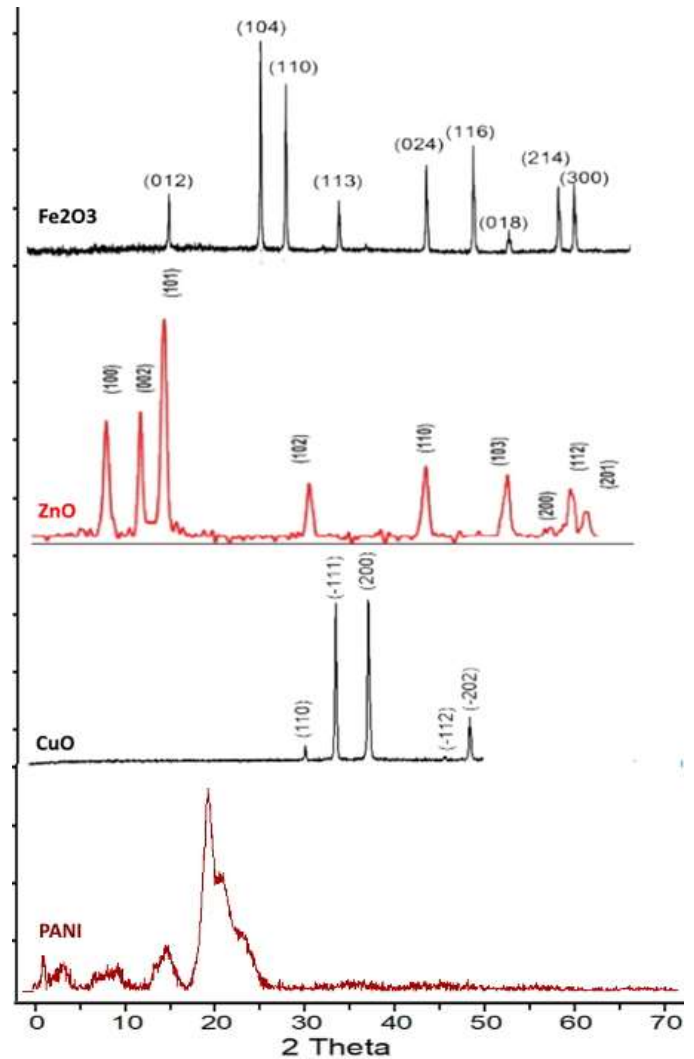


Fig.4: XRD diffraction patterns of PANI, CuO, ZnO and Fe₂O₃.

The hematite phase peaks obtained in the (XRD) pattern of the Fe₂O₃ sample are at $2\theta = 23.15^\circ, 33.21^\circ, 36.11^\circ, 41.17^\circ, 49.31^\circ, 54.12^\circ, 57.20^\circ, 62.35^\circ,$ and 64.10° ; they are associated with levels (012), (104), (110), (113), (024), (116), (214) and (300), respectively. The diffraction peaks are easily assigned to the rhombohedral (hexagonal) structures of the α -Fe₂O₃ phase corresponding to JCPDS number 33-0664 [28].

The XRD patterns of PANI/CuO, PANI/ZnO nanocomposites with the different loading amount of ZnO and CuO (3, 5, and 7%) were shown in Figs. 5 and 6. It can be found that the XRD pattern of the PANI /CuO composite has diffraction peaks around $2\theta \sim 19.29^\circ, 20.782^\circ$ and 26.53° , which are related to (-111), (-102) and (020), respectively. The diffraction peaks in the preferred directions (-111) and (-102) refer to CuO [27] and the peak (020) refers to PANI. It can also be found that the lattice constants a, b and c and the crystallite size of PANI /CuO composite are larger than those of pure CuO and PANI, confirming the formation of nanocomposites (polymer/CuO) by in situ polymerization [29]. It can be seen that the XRD patterns of PANI /ZnO nanocomposites with 7% ZnO content show good crystallinity. This is due to the presence of ZnO nanoparticles and has a significant effect on the diffraction pattern of PANI due to the formation of hydrogen bonds between H-N and oxygen of ZnO [24]. According to Fig. 6, two distinct sharp peaks at $2\theta = 19.28^\circ$ and 26.83° are negligibly shifted with levels (010) and (200), respectively, but their intensity

increases due to the enhancement of ZnO nanoparticles in the matrix PANI. In addition, a peak at $2\theta = 25.44^\circ$ appears with level (102) associated with PANI and its intensity is increased by the addition of ZnO nanoparticles. The XRD results confirm the effect of ZnO nanoparticles in PANI -ZnO nanocomposites, which means that there is an interaction between ZnO nanoparticles and PANI.

However, the XRD pattern of the PANI-Fe₂O₃/ZnO or CuO composite (Figs.5, 6) shows a crystalline phase almost similar to the free Fe₂O₃ with an average particle size, confirming the good enrichment of Fe₂O₃ nanoparticles in the PANI matrix. When comparing the new peaks with JCPDS number 33-0664, they were found to belong to (Fe₂O₃) with a hexagonal phase. With the addition of (Fe₂O₃), an increase in the height and sharpness of the peaks was observed, which led to an increase in the crystallization of the obtained materials. We note a strong preferred orientation of the (104) and (110) planes and a slight shift in the intensity of the peaks, with the PANI-Fe₂O₃/ZnO 7% showing the strongest intensity. All XRD patterns are perfectly aligned with the rhombohedral Fe₂O₃ with unit cell parameters $a=b = 5.036 \text{ \AA}$, $c = 13.75 \text{ \AA}$.

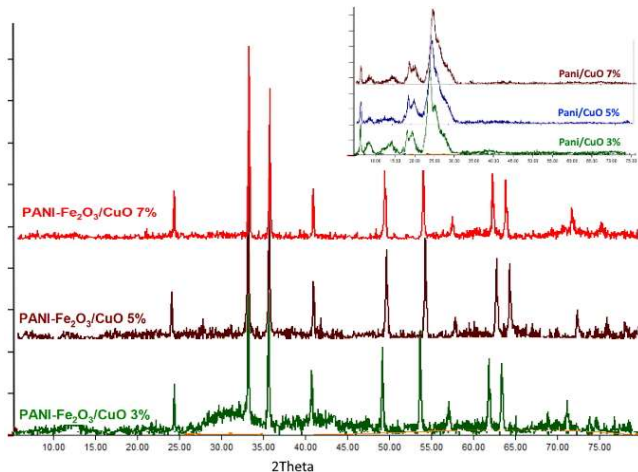


Fig.5: X-ray diffraction patterns of PANI/CuO, PANI-Fe₂O₃/CuO nanocomposites (3, 5, and 7%).

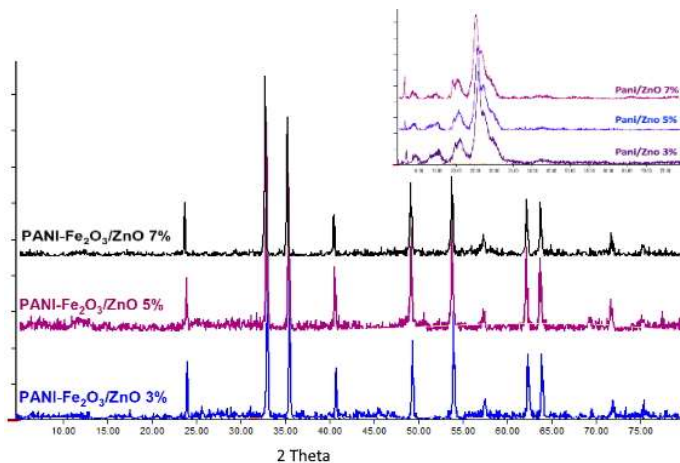


Fig.6: X-ray diffraction patterns of PANI/ZnO, PANI-Fe₂O₃/ZnO nanocomposites (3, 5, and 7%).

We note an increase in intensity as the weight percentage increases, i.e. PANI-Fe₂O₃/CuO 7% represents the strongest intensity. In the XRD patterns of the nanocomposites PANI-Fe₂O₃/ZnO and PANI-Fe₂O₃/CuO, only the peaks associated with the structure of α -Fe₂O₃ can be seen. This confirms the previous results of FTIR, the effect of Fe₂O₃.

III.3. Scanning electron microscopy (SEM)

Figs.7, 8 & 9 showed the surface morphologies of the bulk PANI, PANI/ZnO-7%, PANI/CuO-7%, PANI-Fe₂O₃/CuO-7% and PANI-Fe₂O₃/ZnO-7% nanocomposites. The majority of the grains and flakes in Pani's SEM picture are randomly constructed and have edges. The building also appears to be more porous (Fig.7 (A₁, A₂)). With the use of ImageJ software, the porosity percentage of 31.53% was confirmed. SEM-image (Fig.8 (B & C)) of nano PANI/ZnO-7%, PANI/CuO-7% composites indicate that the incorporation of ZnO & CuO nanoparticles in PANI has a significant effect on the morphology. A decrease in the porosity of PANI can be seen, indicating the dispersion of ZnO & CuO nanoparticles in the PANI matrix. Also, the appearance of certain solid blocks can be seen, which is due to the presence of oxide particles that increase the crystallinity of the composite materials. The micrographs of PANI-Fe₂O₃/CuO-7% and PANI-Fe₂O₃/ZnO-7% (Fig.9 (D & E)) show spherical shapes; PANI-Fe₂O₃/CuO-7% has irregular shapes of grains, while the SEM image of the PANI-Fe₂O₃/ZnO-7% composite shows a completely different picture, where the surface composed of agglomerated, uniform, and spherical grains with a narrow size distribution. This can be attributed to the fact that the Fe₂O₃ nanoparticles act as nuclei during the polymerization of aniline, and cause interaction between the PANI matrix and the oxide particles.

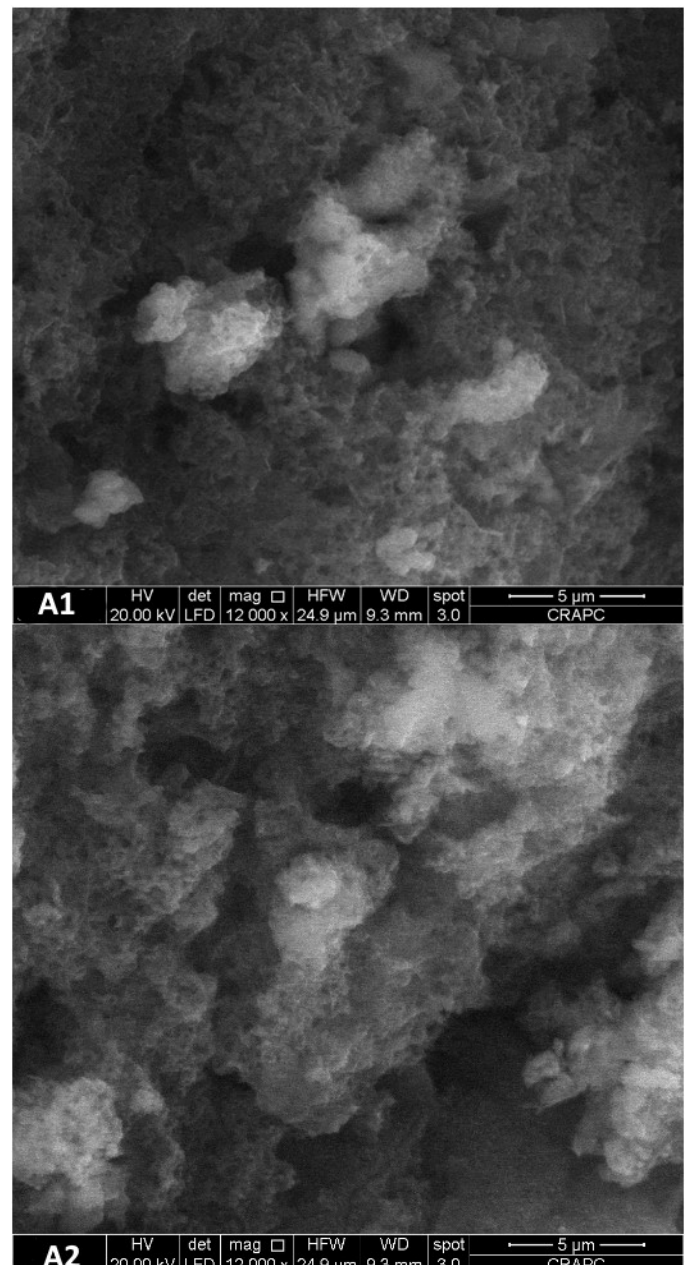


Fig.7: SEM micrograph of: (A₁, A₂) bulk PANI (5 μm).

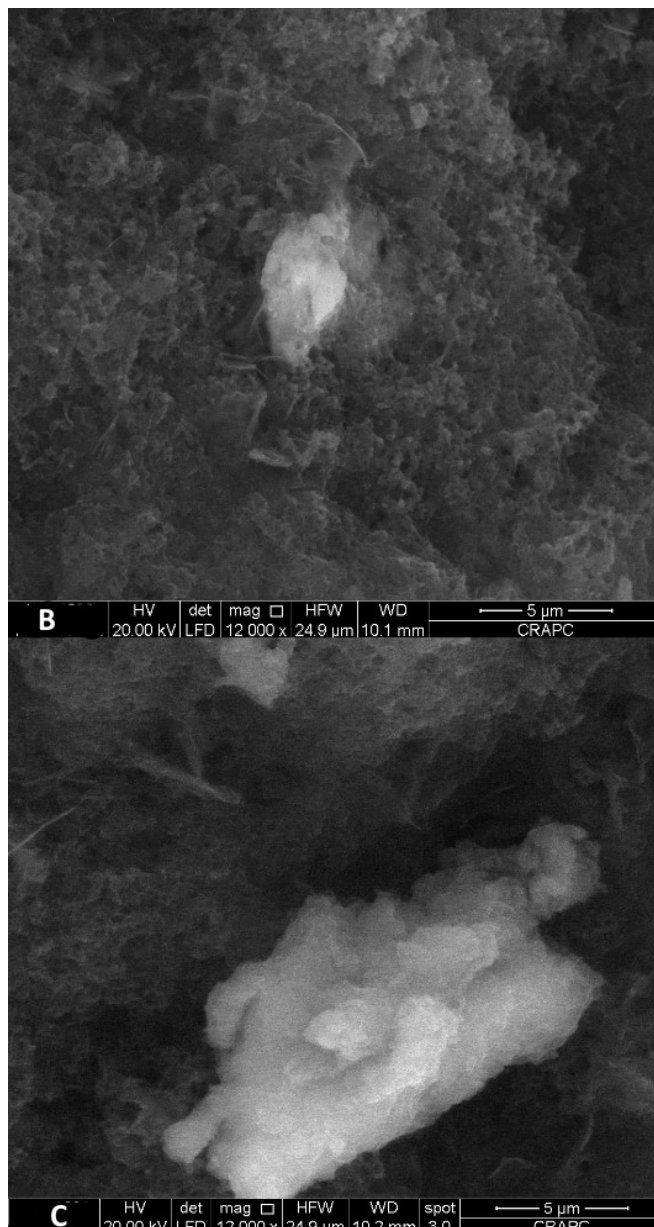


Fig.8: SEM micrograph of: (b) PANI/ZnO 7%, (c) PANI/CuO-7% nanocomposites (at 5um).

III.4. Cyclic voltammetry tests

The cyclic voltammetry (CV) curves of bulk PANI and PANI/ZnO, PANI/CuO, PANI-Fe₂O₃/CuO and PANI-Fe₂O₃/ZnO samples with the weight of ZnO/CuO (7%) were shown in Figs. 10 & 11.

Several factors may influence the course of electropolymerization by changing its potential. Thus includes the electrolyte concentration, the potential range (especially positive limit), the potential scan rate and the electrode material.

The cyclic voltammograms (Fig.10) show two anodic peaks at positive potentials, observed at $E_{pa1} = -0.638$ V and $E_{pa2} = 0.135$ V, respectively, and two cathodic peaks at negative potentials, observed at $E_{pc1} = -0.743$ V and $E_{pc2} = 0.139$ V, corresponding to different oxidation and reduction states of PANI. The first redox peak corresponds to the transition from leucoemeraldine (LE) to emeraldine (EM), and the second redox peak indicates the transition from EM to pernigraniline (PG). The CV shape of the bulk PANI is similar to that of the literature [30].

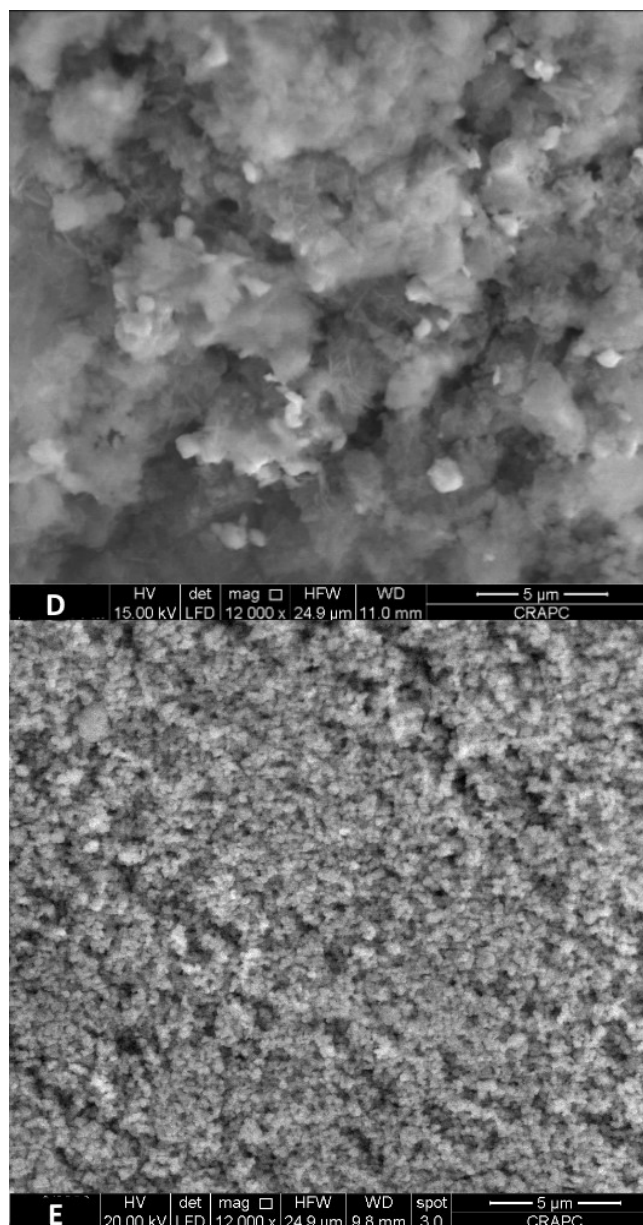


Fig.9: SEM micrograph of: (d) PANI-Fe₂O₃/CuO-7% and (e) PANI-Fe₂O₃/ZnO-7% nanocomposites

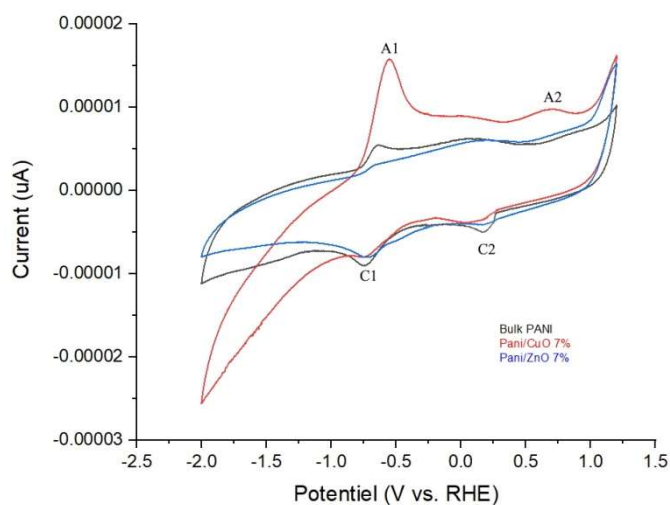


Fig. 10 Cyclic voltammograms recorded in DMSO with TBAPF6 as the supporting electrolyte of: bulk PANI, PANI/CuO (7%) and PANI/ZnO (7%) nanocomposites. Scan rate 50 mV s⁻¹.

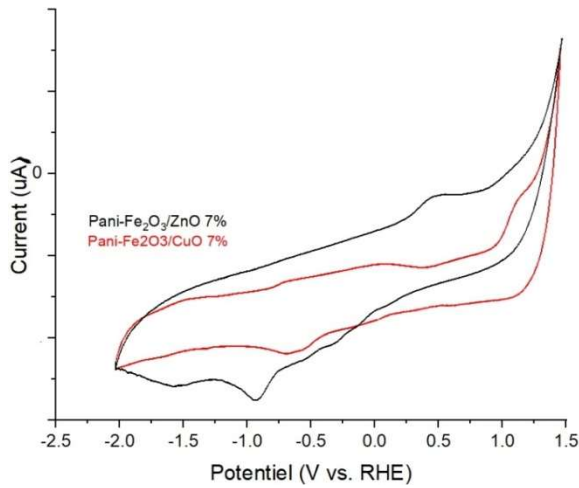


Fig. 11 Cyclic voltammograms recorded in DMSO with TBAPF6 as the supporting electrolyte of: PANI-Fe₂O₃/CuO (7%) and PANI-Fe₂O₃/ZnO (7%) nanocomposites. Scan rate 50 mV s⁻¹.

The CVs of PANI /ZnO and PANI /CuO nanocomposites in Fig.10 show the same shape as those of bulk PANI, but with a decrease in the current intensity of the cathodic and anodic peaks. A slight decrease was observed in the presence of ZnO nanoparticles, but it was particularly pronounced for CuO nanoparticles. This phenomenon was accompanied by a slight shift of the cathodic peak potential toward more positive values, which can be attributed to the modification of the surface electrode by incorporating CuO and ZnO nanoparticles into the PANI.

Therefore, the dispersed CuO, ZnO and Fe₂O₃ affect the electrochemical deposition and properties of PANI (Fig.11). In the case of PANI-Fe₂O₃/CuO (7%) shows three oxidation and three reduction peaks. First oxidation peak represents polyleucoemeraldine (-0.668 V) which is oxidized at more positive potentials to the half oxidized polyemeraldine (0.150 V) and then to the pernigraniline (1.173 V). On the reversing potential, the pernigraniline (-0.638 V) is first reduced to the polyemeraldine radical (-0.0524V) and finally to the fully reduced polyleucoemeraldine (0.069V), while the CV of indicates a pair of redox peak at (0.635, -0.856 V), with a potential peak separation ΔE_p close to 228 mV and is the lowest among the ΔE_p values observed. This confirms that the redox reaction of leucoemeraldine-emeraldine couple became more reversible on PANI-Fe₂O₃/ZnO (7%) compared to PANI-Fe₂O₃/CuO (7%). Notably, this shift and move of redox peaks process was attributed to the PANI structure changes on ZnO and Fe₂O₃ nanoparticles by preparation method, and changed its electrochemical activity.

III.5. UV-vis and Optical properties

The reflectance spectra of all the materials prepared are shown in Fig. 12. They were used to analyze the energy band gap and the nature of the electronic transitions. The absorption edges around 720 nm indicate that the products have good crystallinity [31], which is due to the direct transition of electrons and designates the material as a direct band gap material. The Kubelka-Munk diagrams for these materials are shown in Fig. 13. The reflectance diagrams clearly show that as the CuO content increases, the reflectance of the products also increases, while the reverse is true for ZnO. The extrapolation of the linear range can be used to estimate the band gap energies (E_g), as shown in Fig. 13. The optical band gap is determined by the Kubelka-Munk method [K-M or F(R)]. The K-M method is based on the following equation.

$$F(R) = (1-R)/2R \quad (1)$$

Where R is the reflectance; F(R) is proportional to the extinction coefficient (α). The basic K-M method assumes the diffuse illumination of the particulate coating [32]. A modified K-M function can be obtained by multiplying the F(R) function by hv using the corresponding coefficient (n) associated with an electronic transition as follows

$$[F(R) \times hv]^n \quad (2)$$

The band gap of semiconductor particles can be obtained by plotting this equation as a function of the photon energy in eV. In a different way, several authors applied the K-M method for calculating energy band gap (E_g). Yeredla reported the modified K-M function and plotted as [F(R) hv]² versus photon energy hv or [F(R) hv]^{1/2} versus photon energy hv. This kind of representation is known as the Tauc method [33]. The figure 11 shows the graphical representation of the modified Kubelka-Munk: photon energy hv versus [F(R) hv]². To determine the energy band gap of the obtained nanomaterials, the modified K-M function is applied. According to the Tauc plot, the value of the energy band gap for the products PANI-Fe₂O₃/CuO (3%), PANI-Fe₂O₃/CuO (5%), PANI-Fe₂O₃/ZnO (3%) and PANI-Fe₂O₃/ZnO (5%) was calculated to be 1.426 eV, 1.436 eV, 1.418 eV and 1.464 eV, respectively. It can be seen that the band gap of all products decreases with decreasing molar concentration. The change in band gap is indicative of the change in absorption of the coordinate complex formed between CuO/ZnO-Fe₂O₃ and the PANI chains, which show a decreasing trend due to the lower concentration of CuO/ZnO nanoparticles in the nanocomposites, although ZnO-based compounds outperform CuO in some cases.

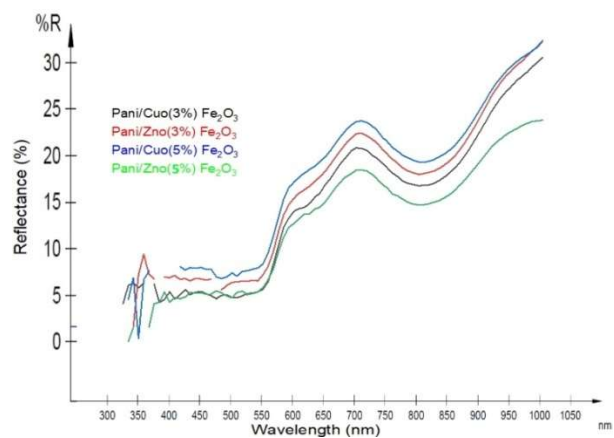


Fig. 12 UV-Vis diffuse reflectance spectrum of: PANI-Fe₂O₃/CuO (3, 5%) and PANI-Fe₂O₃/ZnO (3, 5%) nanocomposites.

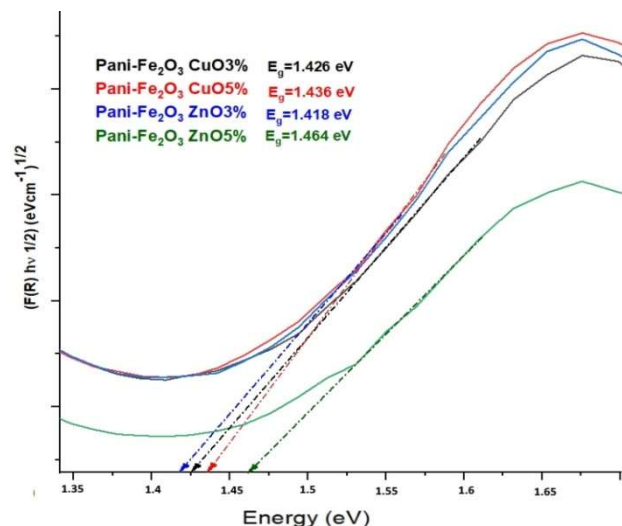


Fig. 13 Graphical representation of modified Kubelka-Munk: photon energy hv versus [F(R) hv]²

IV. CONCLUSION

A series of PANI /CuO, PANI /ZnO, PANI-Fe₂O₃/CuO, PANI-Fe₂O₃/ZnO hybrid materials with the different loading amount of ZnO and CuO (3, 5, and 7%) were prepared by In-Situ polymerization method at 0°C. The synthesized hybrid nanomaterials were analyzed by different techniques. The analyses of FT-IR, XRD, SEM and CV confirmed the formation of CuO/ZnO nanoparticles within the polyaniline matrix and proved the presence of some interaction between ferric particles and PANI. The addition of ferric oxide (Fe₂O₃) nanoparticles did not damage the backbone structure of PANI. XRD results of composites confirmed the rhombohedral (hexagonal) structures of the α -Fe₂O₃ in the amorphous structure of PANI. The XRD and SEM results approved that append of CuO/ZnO and ferric oxide results in increase of the crystallinity of hybrid materials. SEM analysis of the PANI-Fe₂O₃/ZnO-7% demonstrated different morphology to other samples, which has agglomerate, uniform and spherical grains. The electrochemical experiments showed all samples are electroactive and the ox/red properties were very important when the ZnO/CuO content is 7%. The corresponding Tauc's plots show the shift in the band gap with an increase in the concentration of CuO/ZnO in the nanocomposites. In summary, the result can clarify well that Fe₂O₃ act as significant agent. It can be referring to that specific properties can be tailored in the nanomaterials by mixing different proportions of ZnO/CuO nanoparticles. Because of these properties, the obtained nanocomposite may find application in electrical an new biological, chemical and environmental sensors.

ACKNOWLEDGMENT

This work was supported by the scientific and technical research center of physico-chemical analyzes (CRAPC), the directorate general of scientific research and technological development (DGRSDT).

FZ. Zeggai would like to thank Pr. AZZEDINE BOUSSEKSOU for his help and advice.

REFERENCES

- [1] Z. A. AlOthman, M. M. Alam, M. Naushad, & R. Bushra. Electrical conductivity and thermal stability studies on polyaniline Sn (IV) tungstomolybdate nanocomposite cation exchange material: application as Pb (II) ion-selective membrane electrode. *Int. J. Electrochem. Sci.*, vol. 10, no. 3, pp. 2663-2684, Jan. 2015, DOI: <http://dx.doi.org/10.1016/j.jiec.2014.05.022>
- [2] Z. Sun, L. Zhao, H. Wan, H. Liu, D. Wu, & X. Wang. Construction of polyaniline/carbon nanotubes-functionalized phase-change microcapsules for thermal management application of supercapacitors. *Chemical Engineering Journal*, vol. 396, pp.125317, Sep. 2020, DOI: <https://doi.org/10.1016/j.cej.2020.125317>
- [3] H. Wang, J. Lin, & Z. X. Shen. Polyaniline (PANi) based electrode materials for energy storage and conversion. *Journal of science: Advanced materials and devices*, vol. 1, no. 3, pp.225-255, Sep. 2016, DOI: <https://doi.org/10.1016/j.jsamd.2016.08.001>
- [4] Q.A. Alsulami, & A. Rajeh, A. Structural, thermal, optical characterizations of polyaniline/polymethyl methacrylate composite doped by titanium dioxide nanoparticles as an application in optoelectronic devices. *Optical Materials*, vol. 123, pp.111820, 2022, DOI: <https://doi.org/10.1016/j.optmat.2021.111820>
- [5] E. Song, & J. W. Choi. Conducting polyaniline nanowire and its applications in chemiresistive sensing. *Nanomaterials*, vol. 3, no. 3, pp.498-523, Aug. 2013, DOI: <https://doi.org/10.3390/nano3030498>
- [6] K. Crowley, M. R. Smyth, A. J. Killard, & A. Morrin. Printing polyaniline for sensor applications. *Chemical papers*, vol. 67, no. 8, pp. 771-780, Aug. 2013, DOI: <https://doi.org/10.2478/s11696-012-0301-9>
- [7] S. Sathiyarayanan, S. S. Azim, & G. J. E. A. Venkatachari. A new corrosion protection coating with polyaniline-TiO₂ composite for steel. *Electrochimica acta*, vol. 52, no. 5, pp.2068-2074, Jan. 2007, DOI: <https://doi.org/10.1016/j.electacta.2006.08.022>
- [8] P. Simon, Y. Gogotsi. Materials for electrochemical capacitors. *Nature materials*. vol. 7, no 11, pp. 845–854, Nov.2008, DOI: <https://doi.org/10.1038/nmat2297>
- [9] J. Ding, & L. Cheng. Core-shell Fe₃O₄@ SiO₂@ PANI composite: Preparation, characterization, and applications in microwave absorption. *Journal of Alloys and Compounds*, vol.881, pp. 160574, Nov. 2021, DOI: <https://doi.org/10.1016/j.jallcom.2021.160574>
- [10] J. C. Tristão, F. Magalhães, P. Corio, & M. T. C. Sansiviero. Electronic characterization and photocatalytic properties of CdS/TiO₂ semiconductor composite. *Journal of Photochemistry and Photobiology A: Chemistry*, vol. 181, no. 2-3, pp.152-157, Jul. 2006, DOI: <https://doi.org/10.1016/j.jphotochem.2005.11.018>
- [11] N. Rahman, J. Yang, M. Sohail, R. Khan, A. Iqbal, C. Maouche, ... & A. Khan. Insight into metallic oxide semiconductor (SnO₂, ZnO, CuO, α -Fe₂O₃, WO₃)-carbon nitride (g-C₃N₄) heterojunction for gas sensing application. *Sensors and Actuators A: Physical*, vol. 332, pp. 113128, Dec. 2021, DOI: <https://doi.org/10.1016/j.sna.2021.113128>
- [12] N. Tokmoldin, N. Griffiths, D. D. Bradley, & S. A. Haque, A Hybrid Inorganic–Organic Semiconductor Light-Emitting Diode Using ZrO₂ as an Electron-Injection Layer. *Advanced Materials*, vol. 21, no. 34, pp. 3475-3478, Sep. 2009, DOI: <https://doi.org/10.1002/adma.200802594>
- [13] S. Daikh, F.Z. Zeggai, A. Bellil, A. Benyoucef. Chemical polymerization, characterization and electrochemical studies of PANI/ZnO doped with hydrochloric acid and/or zinc chloride: differences between the synthesized nanocomposites. *J. Phys. Chem. Solids* vol. 121, pp. 78–84, Oct. 2018, DOI: <https://doi.org/10.1016/j.jpcs.2018.02.003>
- [14] D. Ouis, F.Z. Zeggai, A. Belmokhtar, A. Benyoucef, B. Meddah, K. Bachari, Role of p-benzoquinone on chemically synthesized nanocomposites by polyaniline with V₂O₅ nanoparticle. *J. Inorg. Organomet. Polym. Mater.* Vol. 30, p. 3502-3510, Mar. 2020, DOI: <https://doi.org/10.1007/s10904-020-01508-7>
- [15] B.K. Sharma, A.K. Gupta, N. Khare, S.K. Dhawan, H.C. Gupta, Synthesis and characterization of polyaniline-ZnO composite and its dielectric behavior, *Synth. Met.* Vol. 159, no. 5-6, pp. 391–395, Mar. 2009, DOI: <https://doi.org/10.1016/j.synthmet.2008.10.010>
- [16] T.K. Sarma, A. Chattopadhyay, Reversible encapsulation of nanometer-size polyaniline and polyaniline-Au-nanoparticle composite in starch, *Langmuir*, vol. 20, no. 11, pp. 4733–4737, Apr. 2004, DOI: <https://doi.org/10.1021/la0495884>
- [17] G.K. Paul, A. Bhaumik, A.S. Patra, S.K. Bera, Enhanced photo-electric response of ZnO/polyaniline layer-by-layer self-assembled films, *Mater. Chem. Phys.* vol. 106, no 2-3, pp. 360-363, Dec. 2007, DOI: <https://doi.org/10.1016/j.matchemphys.2007.06.013>
- [18] Z. Zhang, X. Li, C. Wang, L. Wei, Y. Liu, C. Shao. ZnO hollow nanofibers: fabrication from facile single capillary electrospinning and applications in gas sensors. *The Journal of Physical Chemistry C*, vol. 113, no 45, pp. 19397-19403, Oct. 2009, DOI: <https://doi.org/10.1021/jp9070373>
- [19] N. Samaele, P. Amornpitoksuk, S. Suwanboon, Effect of pH on the morphology and optical properties of modified ZnO particles by SDS via a precipitation method, *Powder Technol.* vol. 203, no 2, pp. 243-247, Nov. 2010, DOI: <https://doi.org/10.1016/j.powtec.2010.05.014>
- [20] V. Prasad, C. D'Souza, D. Yadav, A.J. Shaikh, N. Vigneshwaran, Spectroscopic characterization of zinc oxide nanorods synthesized by solid-state reaction, *Spectrochim. Acta A Mol. Spectros* vol. 65, no. 1, pp. 173–178, Sep. 2006, DOI: <https://doi.org/10.1016/j.saa.2005.10.001>
- [21] M. Nagaraja, S. Prashanth, J. Pattar, H. M. Mahesh, & K. Rajanna. Polyaniline-CuO nanocomposite: Electrical, structural and sensor properties. *Materials Today: Proceedings*, vol. 49, pp. 1989-1992, Aug. 2021, DOI: <https://doi.org/10.1016/j.matpr.2021.08.154>
- [22] A. Olad, & H. Rasouli. Enhanced corrosion protective coating based on conducting polyaniline/zinc nanocomposite. *Journal of applied polymer science*, vol. 115, no. 4, pp. 2221-2227, 2010, DOI: <https://doi.org/10.1002/app.31320>
- [23] S. S. Umare, & B. H. Shambharkar. Synthesis, characterization, and corrosion inhibition study of polyaniline- α -Fe₂O₃ nanocomposite. *Journal of applied polymer science*, vol. 127, no. 5, pp. 3349-3355, May. 2013, DOI: <https://doi.org/10.1002/app.37799>
- [24] L. Shi, X. Wang, L. Lu, X. Yang, X. Wu. Preparation of TiO₂/polyaniline nanocomposite from a lyotropic liquid crystalline solution, *Synthetic Metals* vol. 159, no. 23-24, pp. 2525–2529, Dec. 2009m DOI: <https://doi.org/10.1016/j.synthmet.2009.08.056>
- [25] M. Guo, P. Diao, and S. Cai. Hydrothermal Growth of Well-Aligned ZnO Nanorod Arrays: Dependence of Morphology and Alignment Ordering upon Preparing Conditions. *Journal of Solid State Chemistry*, vol. 178, no. 6, pp. 1864-1873, Jun. 2005, DOI: <https://doi.org/10.1016/j.jssc.2005.03.031>
- [26] F. Bigdeli, A. Morsali, and P. Retalleau. Synthesis and Characterization of Different zinc (II) Oxide Nano-Structures from Direct Thermal Decomposition of ID Coordination Polymers. *Polyhedron*, vol. 29, no. 2, pp. 801-806, Feb. 2010, DOI: <https://doi.org/10.1016/j.poly.2009.10.027>

- [27] J. Wang, S. He, Z. Li, X. Jing, M. Zhang, Z. Jiang. Synthesis of chrysalis-like CuO nanocrystals and their catalytic activity in the thermal decomposition of ammonium perchlorate. *J Chem Sci* vol. 121, no. 6, pp. 1077–1081, Nov. 2009, DOI: <https://doi.org/10.1007/s12039-009-0122-8>
- [28] L. E. Mathevalaa, L. L. Notoa, B. M. Mothudia, M. Chithambob, M.S. Dhlamini. Structural and optical properties of sol-gel derived α -Fe₂O₃ nanoparticles. *Journal of Luminescence*. Vol. 192, pp. 879–887, Dec. 2017, DOI: <https://doi.org/10.1016/j.jlumin.2017.07.055>
- [29] A. Gok and S. Sen, GÖK. Preparation and characterization of poly (2-chloroaniline)/SiO₂ nanocomposite via oxidative polymerization: Comparative UV–vis studies into different solvents of poly (2-chloroaniline) and poly (2-chloroaniline)/SiO₂. *Journal of applied polymer science*, vol. 102, no 1, pp. 935-943, Jul. 2006, DOI: <https://doi.org/10.1002/app.24266>
- [30] G. D. Khuspe, S. T. Navale, D. K. Bandgar, R. D. Sakhare, M. A. Chougule, B. SnO₂ nanoparticles-modified polyaniline films as highly selective, sensitive, reproducible and stable ammonia sensors. *Electronic Materials Letters*, vol. 10, pp. 191-197, Jan. 2014, DOI: <https://doi.org/10.1007/s13391-013-3096-0>
- [31] T. T. Lun, C. Q. Liu, N. Wang, X. N. Zhai, M. S. Song, Q. Ge, X. Y. Zhan, S. M. Liu, H. L. Wang, W. W. Jiang, W. Y. Ding. Preparation of compact CuO films by sol-gel spin coating technique. *Materials Letters*, vol. 257, pp. 126745, Dec. 2019, DOI: <https://doi.org/10.1016/j.matlet.2019.126745>
- [32] P. Kubelka, F. Munk. An article on optics of paint layers. *Zeitschrift für Technische Physik*, vol. 12, no 593-601, pp. 259-274, Aug. 1931, See also English translation by S. Westin (An article on optics of paint layers, <http://www.graphics.cornell.edu/~westin/pubs/kubelka.pdf>)
- [33] R.R. Yeredla, H. Xu. An investigation of nanostructured rutile and anatase plates for improving the photosplitting of water. *Nanotechnology*, vol. 19, no. 5, pp. 055706, Jan. 2008, DOI: [10.1088/0957-4484/19/05/055706](https://doi.org/10.1088/0957-4484/19/05/055706)



Fatima Zohra Zeggai, born on 24-09-1988 in Mascara, is a PhD scientist at CRAPC research centre in Tipaza – Algeria, a member of the Polymer Chemistry Laboratory – University of Ahmed Ben-Bella Oran1 and an ambassador of Africa Elsevier Algeria. She holds a PhD in Materials Chemistry

and Environment from Mustapha Stambouli-Mascara University. She is a member of the department of oxides and porous materials at CRAPC. For years, her interest is focused on materials chemistry (nanomaterials, nanoparticles, carbon materials, conducting polymers, mesoporous materials, pyrochlore), published in many prestigious international journals.